OPTO-ELECTRONICS REVIEW 8(2), 137–146 (2000)

Active fluoride glasses for laser applications

R. STĘPIEŃ[1*], K. JĘDRZEJEWSKI[1], D. PYSZ[1], K. HARAŚNY[1],
Z. MIERCZYK[2], and M. KWAŚNY[2]

[1]Institute of Electronic Materials Technology
133 Wólczyńska Str., 01-919 Warsaw, Poland
[2]Institute of Optoelectronics, Military University of Technology
2 Kaliskiego Str., 00-908 Warsaw, Poland

The synthesis conditions of fluoride ZBLAN type glasses doped with 1, 2 or 5 mol % of Nd^{3+}, Er^{3+} ions have been presented in this paper. Glasses were melted in special clean "glove box" type chamber, constructed and built in ITME, in controlled atmosphere of clean and dry nitrogen. Synthesised glasses are characterised with good homogeneity, high degree of clarifying, and with negligible tendency to crystallisation in temperature of optical fibres drawing. Investigations of spectral properties, luminescence and lifetime of active ions on excited level in the selected samples of glasses have shown their usefulness for lasers: λ = 1.06, 1.35 μm (Nd^{3+}), 1.55 μm (Er^{3+}). Multimode fibres with core from active glass, coated with FEP Teflon layer, were drawn. At present, research works are conducted on mastering of new technology of two glass layers (core-cladding) manufactured by rotation-casting method and of all-glass optical fibres drawing.

Keywords: fluoride glasses, glass synthesis conditions, rare earth ions (Nd^{3+}, Er^{3+}), active optical glasses, luminescence, laser.

1. Introduction

Currently, fluoride glass fibres offer the best prospect for ultra-low loss optical fibres in the infrared region. Fluoride glasses have various desirable optical characteristics, such as a broad transparency range, low refractive index, small dispersion, low Rayleigh scattering, and ultra-low thermal distortion. Furthermore, theoretical prediction shows that these fluoride glass fibres possess the lowest transmission loss of the infrared optical fibres composed of the glass materials, such as chalcogenide and heavy-oxide glasses [1–4].

Fluorozirconate glasses, which are most resistant to devitrification, always include four or more fluoride components. They possess a relatively wide working range, which is defined here as the difference between the crystallisation temperature T_x and the glass transition temperature T_g, typically of 100–150°C, and thus can be cast into large preforms of high optical quality. The fluorozirconate glasses also show a usefully wide range of compositional flexibility, which allows them to be tailored to a broad range of properties essential for forming of compatible core and cladding materials. These advantages led to increasing activity in fabrication of fluoride glass optical fibres [5–9].

The characteristics of a basic ZBLAN composition are shown in Table 1 and its transmission and fibre attenuation, relative to another materials, is shown in Figs. 1 and 2 [10].

As we know, the location of the fundamental vibrational region and infrared edge in these glasses, coupled with their Rayleigh scattering curve, suggests that intrinsic losses near 0.01 dB/km are possible in such heavy metal fluoride glasses between 2.0 and 3.0 μm [11–16].

The composition of glasses is such trivalent lanthanides are easily incorporated, which makes these glasses good laser hosts. The first fluoride fibre laser was demonstrated at 1.05 μm using Nd as a dopant [17]. Following this work, a lot of new dopants have been investigated and many lazing lines have been reported [18].

In particular, the studies on optical properties of rare-earth ions in fluoride glasses have been carried out on Nd^{3+} [19], Eu^{3+} [20], Er^{3+} [21–25], Tm^{3+} [26,27], Pr^{3+} [28], Ho^{3+} [29,30]. Fluoride fibre lasers using Er^{3+} [31–40], Nd^{3+} [17], Tm^{3+} [41–46], Pr^{3+} [47–49], and Ho^{3+} [50–52] have been demonstrated. Moreover, fibre amplifiers have been presented at 0.8 μm [53,54], 1.3 μm [55–64], 1.5 μm [65–73], and 2.7 μm [40].

It is worth noting that the wavelengths 1.3 and 2.7 μm are especially significant since they are as yet unavailable in silica based fibre. This fact is mainly caused by the low phonon energies (500 cm^{-1}) of the fluoride glass, hosts in comparison with silica glasses, which reduce nonradiative transitions due to multiphonon emission. The relatively low phonon energies also help in obtaining an up-conversion effects in these active glasses leading, e.g., to green and blue light emission [74–81].

*e-mail: rstepien@wa.onet.pl

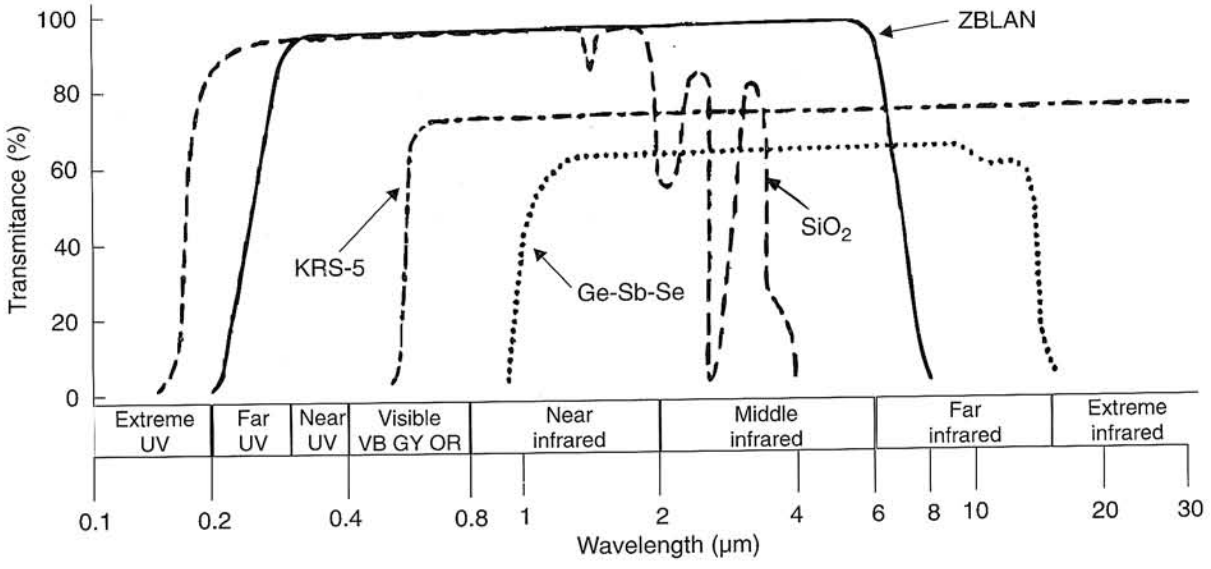

Fig. 1. Transmission curves for various candidate IR fibre materials at a thickness of 5 mm (after Ref. 10).

Table 1. Thermal, mechanical, and optical properties of ZBLAN fluoride glass (after Ref. 10).

Material property	Fluoride glass
Commercial acronym	ZBLAN
Composition (mol %)	$53ZrF_4$–$20BaF_2$–$4LaF_3$–$3AlF_3$–20NaF
Glass transition (T_g) (°C)	260
Specific heat (cal/g°C)	0.151
Thermal conductivity (25°C) (W/m°C)	0.628
Expansion coefficient (25–200°C) ($°C^{-1}$)	17.2×10^{-6}
Density (g/cm^3)	4.33
Knoop hardness (kg/mm^2)	225
Fracture toughness (K_{1c}) (MPa $m^{1/2}$)	≈ 0.32
Poisson's ratio	0.17
Elastic moduli (GPa):	
Young's	58.3
Shear	20.5
Bulk	47.7
Refractive index	1.499 (0.589 μm)
Abbe number	76
Zero material dispersion wavelength (μm)	1.6
Non-linear index (n_2)	0.85×10^{-13}
Temperature coefficient of refractive index (dn/dT) ($°C^{-1}$)	-14.75×10^{-6}
Approximate transmission range (1 mm thickness, T > 10%) (μm)	0.22–8.0

Great interest in fluoride Nd^{3+}, Er^{3+}, Pr^{3+} doped glasses observed in recent years is first of all due to their possible applications as active media of fibre lasers, optical amplifiers, and visible light laser system of "up-conversion" type [83,84].

Fluoride glasses, in comparison with typical silica glasses used in fibreoptic telecommunication, are characterised by low attenuation of radiation in the range of significantly wider wavelengths [84]. Different energetic structure of these glasses and low energies of phonons [85], in comparison with commonly used silica, silicate, and phosphate glasses make possibility of significant number of quantum transitions of high efficiency when glasses are doped with rare earth ions, especially within the range of longer wavelengths. It results from the literature data that many of those radiant transitions were observed only in glasses based on pure fluorides [10,18].

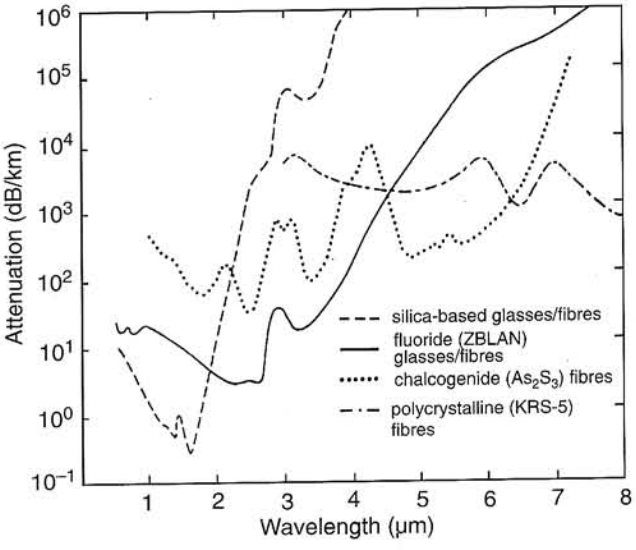

Fig. 2. Attenuation vs. wavelength for several IR transmitting optical fibres (after Ref. 15).

Fluoride glasses doped with rare earth ions can be widely applied in telecommunication, optoelectronics, medicine, and environmental protection. Especially, about the possible applications of these glasses in telecommunication testifies the obtained amplification of radiation for wavelengths of 0.8, 1.06, 1.3, and 1.54 μm [86,87] used in telecommunication windows of minimal attenuation for silica being the most frequently used as fibre transmitting medium. A wavelength of 1.3 μm is interesting because till now there is lack of amplifiers that are enough quantum efficient to be used in majority of already performed fibreoptic lines.

Fluoride amplifiers for 1.55 μm are considered by some manufacturers as more advantageous because their bands are much wider and plane what is good for application of many amplifiers set in cascade system or DWDM dense multiplexing that is now extensively developed.

Possibility of optical amplification within the range of wavelength of 2.7 μm [88] is promising for performance of high power source applied as surgical instrument due to very strong absorption by OH^- ions within this range of wavelengths. In many laboratories in the world, researchers obtained significant experience in performance of coherent fibre sources of a power of several watts for continuous operation and several kilowatts for pulse operation with no thermal and optical degradation of a fibre.

The aim of the works carried out in the Institute of Electronic Materials Technology (ITME) in Warsaw, Poland, was to construct special technological apparatus and making synthesis of active fluoride glass of ZBLAN type that is recommended type of fluoride glass due to its optical properties. Elaboration of synthesis and laboratory manufacturing of Nd^{3+}, Er^{3+} doped fluoride glasses is the base for further searching for other constitutions of this type of glasses with new components that enable obtaining new radiant transitions, especially of continuous bands of tuned coherent sources, and increase in quantum efficiency for wavelengths used in practice.

2. Synthesis of glasses

As optimal constitution of fluoride matrix glass, a glass based on fluorozirconate of molecular composition of $53ZrF_4 + 20BaF_2 + 4LaF_3 + 3AlF_3 + 20NaF$, known as ZBLAN glass, was chosen. It is the most stable fluoride glass system, resistant to crystallisation during its secondary heating up to softening temperature when glass is pulled as a fibre.

Doping of fluoride glasses with rare earth ions was limited to two compounds: neodymium and erbium fluorides. Fluoride compounds of the FluortranR (fibre grade) MERC firm were used for glass synthesis.

Among the raw materials used for melting process only ZrF_4 is fusible material, $T_{mel} \cong 600°C$. Other crystals have melting temperature over 1000°C: BaF_2–1280°C, LaF_3–1493°C, AlF_3–1291°C, NaF–988°C, NdF_3–1410°C, and ErF_3–1380°C. Actually these crystals are slowly dissolved in ZrF_4 liquid. Thus, there is a necessity of long–lasting keeping of a melt at high temperature until total crystals dissolving. It is also the reason of higher volatility of ZrF_4 because the pressures of steams of particular components, as a function of temperature, are similar. Volatility of ZrF_4 was corrected by adequate addition of this component to raw material in the amount resulting from molecular composition.

Special facility for fluoride glasses melting (Fig. 3) was constructed and performed in the ITME. The objective for building this separate glove box was to allow complete processing of the glasses within inert environment. The pro-

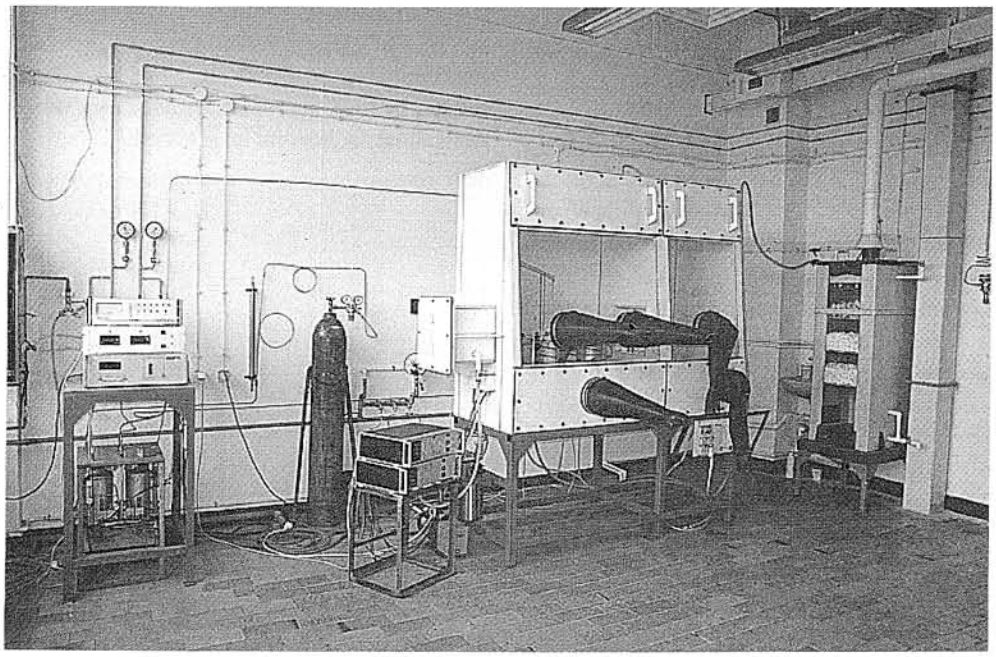

Fig. 3. Fluoride glass melting laboratory of the Institute of Electronic Materials Technology, Warsaw, Poland.

cessing was to include storage of raw materials and weighing and batching of powders, but in addition it was to include melting of the glasses without contacting the environment, as well as casting and annealing under these same inert conditions. In other words, ambient conditions were to be avoided at all times and only the completed annealed glass or preform was to be allowed to come into contact with air. Previous experiments with glasses cast under ambient conditions have shown that OH can be incorporated at this stage.

The glove box assembly, shown on photography, has two separate glove boxes connected by a transfer port. These boxes were constructed on the base of stainless steel framework and have walls made of PVC plates. One glove box is used for storage, weighing, and batching of powders, while the other is used for melting, casting, and annealing. In this way, fine powders that were emitted into the glove box during batching would not contaminate the melting environment.

The both melting and annealing furnaces are positioned in the second glove box. Furnaces and glove box bottom is water-cooled, what allowed the heat from the furnaces to be exhausted from the box volume. The gases from reactive glove box went through the scrubber. The both furnace are a kanthal wound resistance type, using an alumina mandrel and was controlled to ±2°C using a thermocouple located in the melt enclosure. The melting crucible containing the batch could be transferred into the melting glove box from the batching box through the transfer port. It could then be lowered into the melting enclosure using the special arrangement. The crucible was supported on a ceramic pedestal.

The starting materials were in general anhydrous fluorides apart from a small amount of NH_4HF_2 incorporated into the batch to convert any residual oxides present in the raw materials as impurities. All materials were stored in one of the glove boxes to prevent hydrolysis. The glove box was flushed with dry nitrogen supplied from a liquid nitrogen source. The internal pressure of the box was always above atmospheric and generally about 30 mm of water. The glove box was also used for batching and weighing so that all processing up to the melting stage was done under inert conditions. Some powders such as BaF_2 are supplied in large crystalline lumps, which have to be broken up for accurate weighing. These materials were therefore ground using an agate mortar and pestle. Batch sizes varied according to the required volume of glass but in general were in the region 10–40 g. Glasses were melted in platinum crucible. A lid was placed over crucible in order to reduce volatilisation (mainly ZrF_4) and the size of the crucibles was 35 mm maximum outer diameter with a depth of 38 mm. The batch was transferred to the melting crucible inside the glove box, prior to insertion in the furnace so minimising exposure to ambient one. Normally 1.0 g of NH_4HF_2/10 g glass melt was also added. An example of a typical batch for melting basic ZBLAN type glass was

ZrF_4 19.11 g, BaF_2 7.38 g, LaF_3 1.65 g, AlF_3 0.54 g, NaF 1.77 g

to give a total weight of 30 g. In addition, 0.45 g of extra ZrF_4 was added to make up for volatilisation.

A typical melting schedule was as follows.

Time (h)	Temperature (°C)
0–0.5	230
0.5–0	230–400
0.75–1.25	400
1.25–2.0	400–760
2.0–5.0	760
5.0–5.5	760–630
5.5–6.0	630
6.25	Caste

The initial hold at 230 and 400°C was to allow fluorination and the temperature was then raised to 760°C to allow fusion and melting and left for a period to allow homogenisation. Any remaining NH_4F was at this stage sublimed out of the batch to condense on the upper cooler part of the furnace. The hold at this higher temperature was limited in time to avoid excessive volatilization of ZrF_4. Next the melt was cooled to 630°C to reduce the heat required to be removed from the melt during the final caste and quench. This temperature was chosen since it was above the melt liquidus so that the glass would not crystallise at this stage.

To remove glass stress, the annealing furnace was first heated up to temperature of 290–300°C. After heating and keeping at this temperature for one hour, temperature was reduced down to 220–260°C. After casting, the sample in a mould was placed into a furnace again and underwent annealing process for about 0.5 hour at temperature 220–260°C, next it was cooled to room temperature with the speed of 1–2°C/min.

Such a melting process made it possible to obtain the samples of glass in form of rods of diameter of 10 mm and maximal length of 100 mm (Fig. 4). Glasses were characterised by high homogeneity and there were no gaseous and crystalline inclusions inside them.

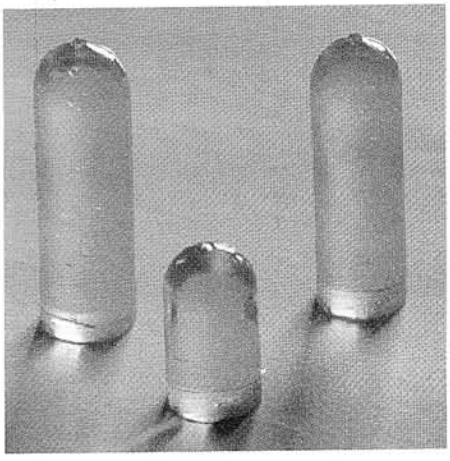

Fig. 4. Fluoride ZBLAN type glasses doped with NdF_3 (1 and 5 mol %), ErF_3 (1 mol %).

3. Examination of glass properties

Dilatometric measurements were made that consisted in determination of a coefficient of linear thermal expansion $\alpha = (185\pm2)\times10^{-7}$ K^{-1} for temperature range 20–200°C, transformation temperature $T_g = 259 \pm 5$°C and dilatometric softening point DSP = 282±5°C. Moreover, refractive index has been determined and its value was $n_d = 1.497$.

In order to determine dependence of absorption coefficient on wavelength $k(\lambda)$ for the investigated samples, the measurements of transmission, as a function of wavelength, were performed. Measurements were carried out within the spectral range of 200–1100 nm ($\Delta\lambda$ = 1 nm) using LAMBDA2 PERKIN ELMER spectrophotometer, within the range of 1100–1500 nm ($\Delta\lambda$ = 1 nm) using ACTA MVII BECKMAN spectrophotometer, and within the range of 1500–25000 nm ($\Delta 1/\lambda$ = 1 cm^{-1}) using Fourier PERKIN ELMER spectrophotometer 1725–X FT–IR.

On the basis of the measurements of samples transmission $T(\lambda)$, an absorption coefficient was calculated with consideration of multiple reflections of radiation inside a sample

$$k(\lambda) = \frac{1}{d} \ln \frac{1}{T_r(\lambda)}, \tag{1}$$

where

$$T_r(\lambda) = \frac{\sqrt{(1-r_f)^4 + 4r_f^2 T^2(\lambda)} - (1-r_f)^2}{2T(\lambda)r_f^2}, \tag{2}$$

$T(\lambda)$ is the measured value of sample transmission, d is the sample thickness, r_f is the Fresnel reflection coefficient.

Spectral curves of absorption coefficient for Nd^{3+}, Er^{3+} doped glasses, determined for wavelengths of 200–8200 nm, are shown in Figs. 5 and 6.

Measurements of luminescence spectrum for the samples of fluoride Nd^{3+}, Er^{3+} doped glasses have been performed using the system presented in Fig. 7. In the excitation channel the following laser sources were applied:

- diode laser emitting radiation at 810 nm (Nd^{3+} doped glasses),
- diode laser emitting radiation at 970 nm (Er^{3+} doped glasses).

For laser action, among other features, there must be a strong fluorescence at the required wavelength. Fluorescence spectra of rare–earth ions in the glass host are therefore very useful, firstly, to identify possible pump-bands and secondly, in identifying possible lasing wavelength.

Luminescence excited with laser radiation, after spectral splitting, in H20 (JOBIN YVON) monochromator was registered by means of LOCK-IN (STANFORD RESEARCH SR510) system with thermoelectrically cooled InGaAs detector. Luminescence curves are presented in Figs. 8 and 9.

Measurements of lifetime at the upper laser level for the samples of ZBLAN (1%, 2%, and 5% NdF_3) and ZBLAN (1% ErF_3 and 2% ErF_3) were made by means of direct method with pulse excitation. The investigated medium was excited with radiation pulse duration significantly shorter than the lifetime τ at the excited level. After excita-

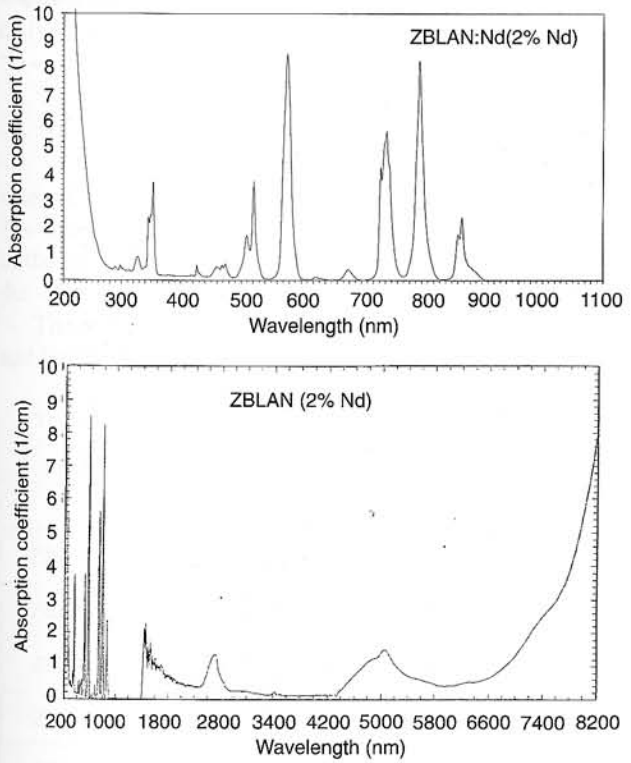

Fig. 5. Absorption curves of neodymium doped ZBLAN glass.

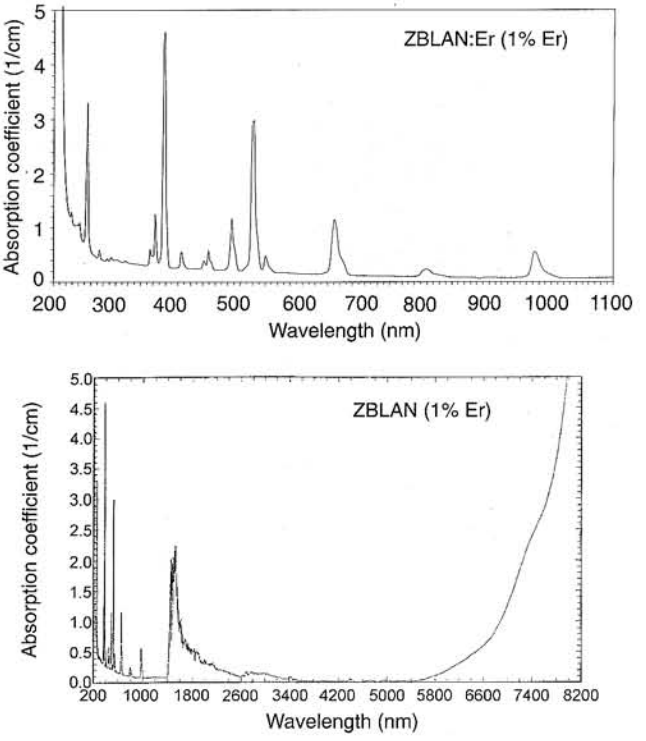

Fig. 6. Absorption curves of erbium doped ZBLAN glass.

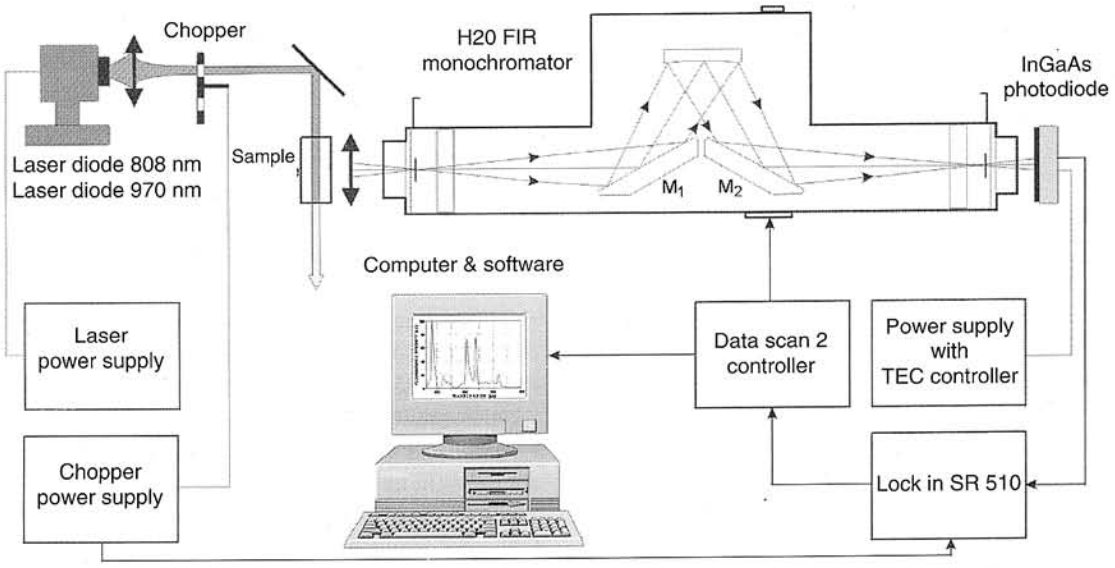

Fig. 7. Scheme of measuring system with H20 monochromator used for determination of luminescence spectra of the examined glasses.

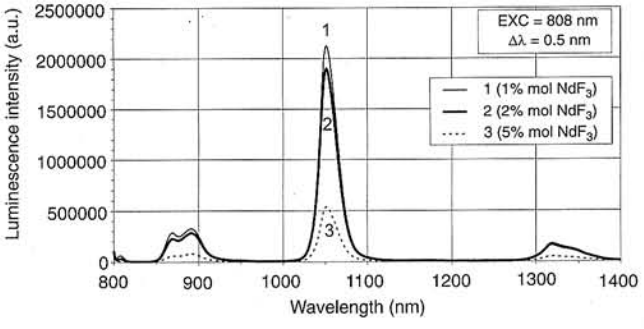

Fig. 8. Luminescence curves of neodymium doped ZBLAN glasses.

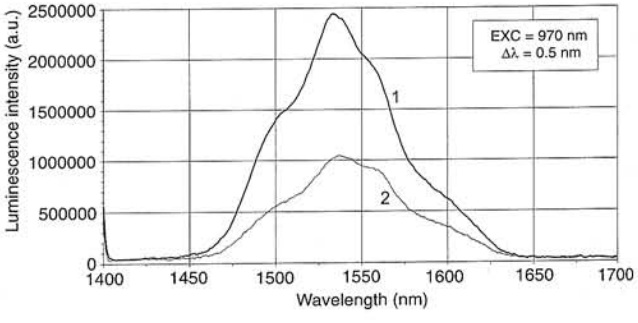

Fig. 9. Luminescence curves of erbium doped ZBLAN glasses 1–1 mol %, 2–2 mol % of ErF_3

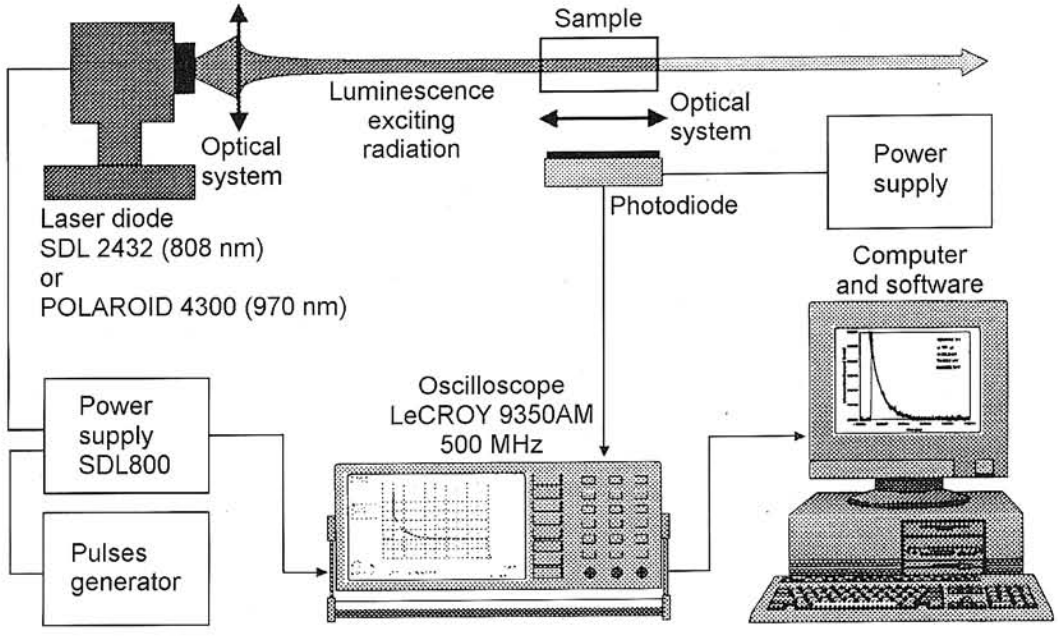

Fig. 10. Scheme of experimental set–up for measurements of fluorescence decay.

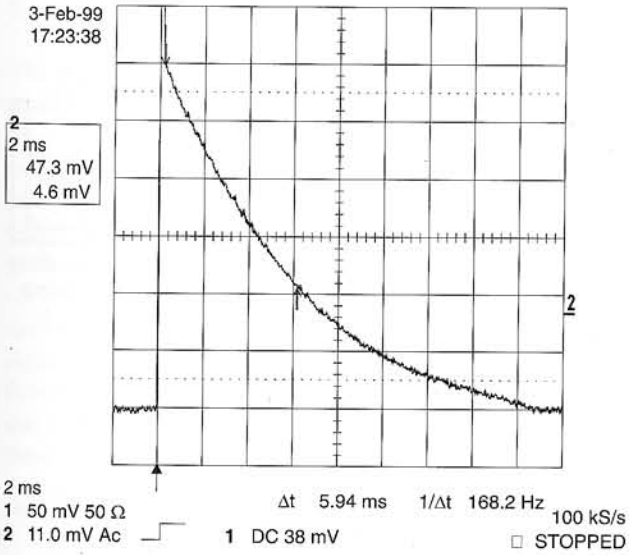

Fig. 11. Oscillogram of temporal course of fluorescence decay in the ZBLAN+2 mol % ErF_3 glass sample.

tion a population level decay occurs the evidence of which is fluorescence decay that can be observed.

A source of diagnostic pulses of wavelength 808 nm (excitation of Nd^{3+} ions) was SDL2432 diode laser and the pulses of 970 nm wavelengths (excitation of Er^{3+} ions) was diode laser POLAROID 4300 (Fig. 10).

Figure 11 presents temporal course of fluorescence decay in the ZBLAN+2 mol % ErF_3 glass sample.

The obtained measurement results of the fluorescence intensity (I) versus the time (t) were approximated numerically by the following function

$$I = I_0 \exp\left(-\frac{t}{\tau}\right) \tag{3}$$

where I_0 is the initial intensity, and τ is the time–constant. The time-constant τ (fluorescence decay time) corresponds to the time after which the fluorescence intensity I reaches the value equals I_0/e.

The results of analysis of fluorescence decay for Nd^{3+} and Er^{3+} doped glasses are presented in Table 2.

Table 2. Fluorescence decay for neodymium ($^4F_{3/2}$ level) and erbium ($^4I_{13/2}$ level) doped ZBLAN glasses

Glass type	Fluorescence decay
ZBLAN + 1 mol % NdF_3	482 ±5 μs
ZBLAN + 2 mol % NdF_3	387 ±5 μs
ZBLAN + 5 mol % NdF_3	181 ±5 μs
ZBLAN + 1 mol % ErF_3	6.5 ±0.1 μs
ZBLAN + 2 mol % ErF_3	6.7 ±0.1 μs

4. Optical fibre preparation

The techniques used to draw fluoride glass preform into fibre are based on standard methods developed for silica fibre. The main difference is the draw furnace since much lower temperatures are required for fluoride fibres. A schematic of the draw tower is given in Fig. 12. A feeder is used to lower the preform into the furnace at constant rate. The preform is mounted inside a silica liner which is sealed at the top end around the stainless steel rod so that dry nitrogen or argon can be flushed through the chamber. In this way surface crystallisation during reheating of the preform to draw fibre can be kept to a minimum. A diameter monitor is used to measure the fibre diameter, and the output from the monitor is then servo–linked to the winding drum speed controller. In general the diameter of fluoride fibres is more difficult to control than for silica, since the working range is much less. However in most cases diameter fluctuations can be reduced to ±2 μm. Polymer coatings cured by UV light can be applied in the usual way. Essentially, epoxy acrylates can be applied in the liquid.

Multimode optical fibre with core from the synthesised, fluoride active glass coated with FEP Teflon layer have been drawn in ITME using the method, which idea is shown in Fig. 13. A glass rod, 9.55 mm in diameter, after grinding and mechanical as well as chemical polishing was inserted into Teflon FEP tube having 9.6 mm of inner and 11.2 mm of outer diameter and a such preform was pulled to obtain fibre 100–150 μm in diameter.

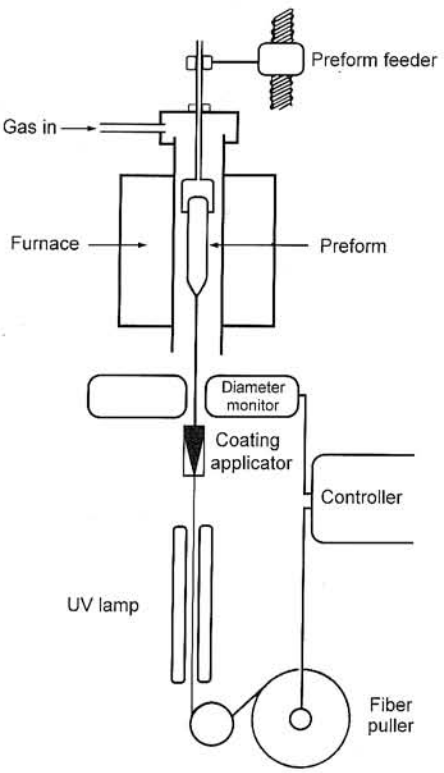

Fig. 12. Scheme of the fluoride glass fibre draw tower (after Ref. 10).

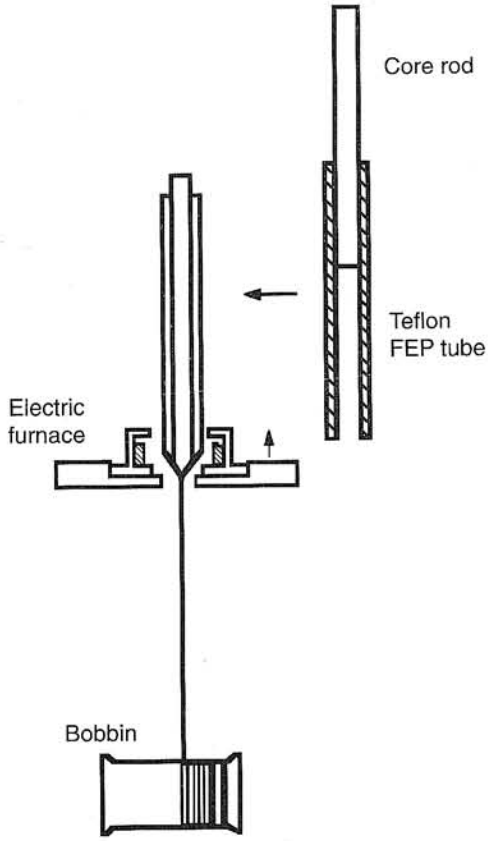

Fig. 13. Drawing method an optical fibre jacketed with Teflon FEP (after Ref. 89).

Now we are getting ready to perform the measurements of absorption, spectroscopic, and laser properties of the obtained fibres. There were fibres without glassy cladding, with organic jacket only. At present, research works are conducted on mastering new technology of two glass layer (core-cladding) preforms manufacturing by rotation-casting method and of all-glass optical fibres drawing.

Two independent casting techniques have been proposed to make core-clad preforms. In first technique termed "built in casting" the molten cladding glass is pouring into a preheated mould and a frozen skin of glass is forming on the inside walls of the mould. The mould is then inverted to allow the molten central volume of the glass to pour out, leaving a cladding glass tube (Fig. 14). The core glass is then poured into this tube to form a preform, and the assembly is cooled and annealed [89].

A second technique, realised in ITME, is based on an old established method used in other glass systems to form tubes by rotational casting. The technique is illustrated in Fig. 15. In this case the mould is only partially filled with molten cladding glass, and then swung to a horizontal position and span until the glass cools to form a tube. In this way more controlled cladding tubes can be fabricated and the core glass is cast into this tube in the usual way [90].

In fibre optics laboratory of ITME a small specially adapted lathe was installed inside the melting glove box so

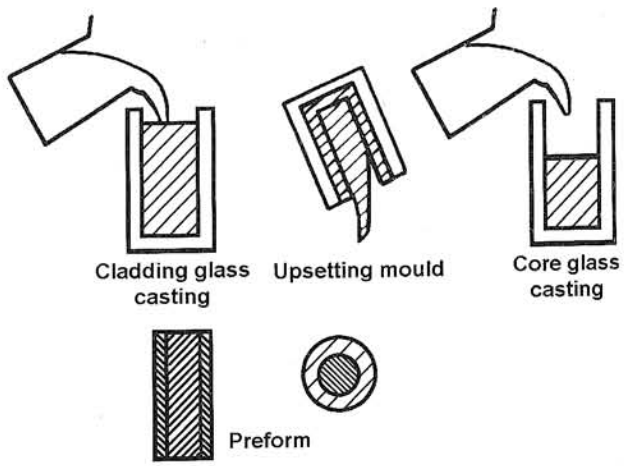

Fig. 14. Schematic of a built–in casting process for a fluoride glass preform (after Ref. 89).

that casting again could be done under inert conditions. A typical spin speed is about 5000 rpm and the glass takes several tens of seconds before solidifying to form a tube. The mould is fabricated in brass and is split along the centre line for easy removal of the preform. The bore of the mould is 10 mm.

After casting the mould is transferred into a separate annealing oven situated near melting oven, again without coming into contact with ambient. The preform was kept for 0.5 h at 260°C and then the temperature was ramped down to room temperature at a rate of max. 2°C/min.

Since the outer surface of the molten glass is brought into contact with a potentially contaminating metal during the casting process, several techniques have been developed to remove the outer layer from the preform. They include mechanical polishing and chemical etching and the techniques are able to improve both the fibre strength and the loss. Frequent problems with this casting technique included the formation of crystals and bubbles in the preform particularly at the core-cladding interface and also at the centre of the preform.

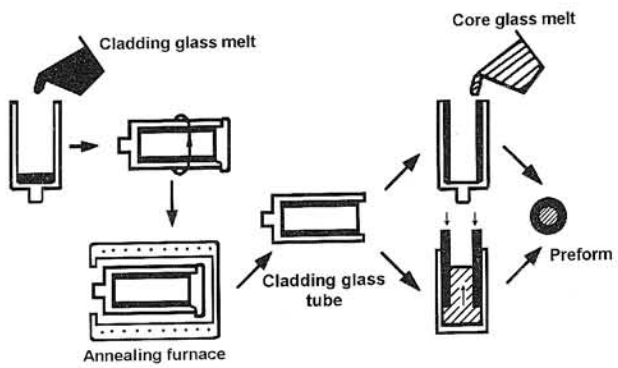

Fig. 15. Rotational casting of fluoride glass preform (after Ref. 90).

5. Conclusions

The conditions of synthesis of fluoride glasses doped with neodymium and erbium, devoted to laser applications, were defined. These are the most promising dopants as far as application in practice is concerned. Having a neodymium doped matrix a laser action can be achieved or amplification of radiation at 1.06 μm wavelength. Erbium fluoride glass is ideal material for laser system generating radiation of wavelength of about 2.8 μm. An optical fibre made of such a material can be a generator or an amplifier of optical signal in surgical instrument. Erbium doped fluoride amplifiers for wavelength of 1.55 μm are more and more popular due to their plane transmission characteristics. Moreover, these dopants can be used for up-conversion effect realisation and laser action achievement within the range of visible light.

The carried out investigations of thermal, optical, and spectroscopic properties of the prepared Nd^{3+}, Er^{3+} fluoride glasses showed their good quality so they can be applied in laser systems.

Acknowledgement

The investigations were made within the frame of project No PBZ–023–10 financed by the State Committee for Scientific Research, Poland.

References

1. T. Miyashita and T. Manabe, IEEE J. *Quantum Electron.* **QE–18**, 1432–50 (1982).
2. M. Poulain, M. Poulain, J. Lucas, and P. Braun, *Mater. Res. Bull.* **10**, 243–246 (1975).
3. K. Ohsawa, T. Shibata, K. Nakamura, and S. Yoshida, Paper 1.1, Technical Digest, *7th European Conference on Optical Communication (ECOC)*, Bella Center, Copenhagen, Denmark, 8–11 September, 1981.
4. K. Ohsawa, T. Shibata, and K. Takahashi, US Patent 4,445,755, 1 May, 1984.
5. P.W. France, PhD Thesis, Sheffield University, 1987.
6. H. Tokiwa, Y. Minura, O. Shinbori, and T. Nakai, *J. Lightwave Technol.* **3**, 569 (1985).
7. D.C. Tran in *Proc. Optical Fibre Communications*, Atlanta, GA, TUA1, 1986
8. P.W. France, S.F. Carter, M.W. Moore, and C.R. Day, *Br. Telecom Technol. J.* **5b**, 28 (1987).
9. T. Kanamori and S. Sakaguchi, *Jpn. J. Appl. Phys.* **6**, 468 (1986).
10. P.W. France, M.G. Drexhage, J.M. Parker, M.W. Moore, and J.V. Wright, *Fluoride Glass Optical Fibres*, Blackie, Glasgow, 1990.
11. C.H.L. Goodman, *IEEE J. Solid State Electron Devices* **2**, 129 (1978).
12. J.R. Gannon, *Proc. SPIE* **266**, 62 (1981).
13. H. Tokiwa, Y. Mimura, O. Shinbori, and T. Nakai, *J. Lightwave Technol.* **3**, 569 (1985).
14. Y. Mimura, H. Tokiwa, O. Shinbori, and T. Nakai, US Patent 4,674,835, 23 June, 1987.
15. P.W. France, S.F. Carter, M.W. Moore, and J.R. Williams, *Mater Sci. Forum* **19–20**, 381 (1987).
16. M.G. Drexhage, C.T. Moynihan, M. Laleh Boulos, and K.P. Quinlan, in *Proceedings of the Conference on the Physics of Fiber Optics*, edited by B. Bendow and S. Mitra, Columbus, Ohio, American Society, 1981.
17. M.C. Brieley and P.W. France, *Electron. Lett.* **23**, 815 (1987).
18. P. Szczepański, "Active fluoride glasses", ITME, *Materiały Elektroniczne* **3**, 52–76 (1994).
19. J. Lucas, M. Chanthanasinh, M. Poulain, P. Brun, and M.J. Weber, *J. Non–Cryst. Solids* **27**, 273 (1978).
20. R. Reisfeld, E. Greenberg, R.N. Brown, M.G. Drexhage, and C.K. Jorgesen, *Chem. Phys. Lett.* **95**, 91 (1983).
21. R. Reisfeld, G. Katz, N. Spector, C.K. Jorgensen, C. Jacoboni, and R. DePape, *J. Solid Chem.* **41**, 253 (1982).
22. R. Reisfeld, G. Katz, C. Jacoboni, R. DePape, M.G. Drexhage, R.N. Brown, and C.K. Jorgensen, *J. Solid Chem.* **4**, 323 (1983).
23. M.D. Shinn, W.A. Sibley, M.G. Drexhage, and R.N. Brown, *Phys. Rev.* B **27**, 6635 (1983).
24. W. Cho, M.M. Kim, J. Jo, and T. Hahn, "Lifetime variation of $^4I_{13/2}$ level of Er^{3+} in fluorozirconate glasses", *Halide Glasses VI*, Clausthal, 1989.
25. H. Yanagita, K. Okada, K. Miura, H. Toratani, and T. Yamashita, "Er^{3+}–fluoro–zirconate–aluminium glasses", *Halide Glasses VI*, Clausthal, 1989.
26. J. Sanz, R. Cases, and R. Alcala, *J. Non–Cryst. Solids* **93**, 377 (1987).
27. C. Guery, J.L. Adam, and J. Lucas, *J. Lum.* **42**, 181 (1988).
28. M. Eyal, E. Greenberg, R. Reisfeld, and N. Spector, *Chem. Phys. Lett.* **117**, 108 (1985).
29. R. Reisfeld, M. Eyal, E. Greenberg, and C.K. Jorgensen, *Chem. Phys. Lett.* **118**, 25 (1985).
30. J.L. Adam, C. Guery, J. Lucas, J. Rubin, B. Moine, and G. Boulon, *Mat. Sc. Forum* **19–20**, 573 (1987).
31. S.A. Pollack and M. Robinson, *Electron. Lett.* **24**, 320 (1988).
32. F. Auzel, D. Meinchennin, and H. Poignant, *Electron. Lett.* **24**, 909 (1988).
33. M.C. Brierley and P.W. France, *Electron. Lett.* **24**, 935 (1988).
34. F. Auzel, D. Meichnenin, and H. Poignant, *Electron. Lett.* **24**, 1416 (1988).
35. R.S. Quimby and W. Miniscalco, *Appl. Opt.* **28**, 14 (1989).
36. J.Y. Allain, M. Monerie, and H. Poignant, *Electron. Lett.* **25**, 28 (1989).
37. J.Y. Allain, M. Monerie, and H. Poignant, *Electron. Lett.* **25**, 1082 (1989).
38. R. Allen, L. Esterowitz, and R.J. Ginther, *Appl. Phys. Lett.* **56**, 1635 (1990).
39. J.Y. Allain, M. Monerie, and H. Poignant, *Electron. Lett.* **27**, 445 (1991).
40. D. Ronarc'h, M. Guibert, F. Auzel, D. Mechenin, J.Y. Allain, and H. Poignant, *Electron. Lett.* **27**, 511 (1991).
41. L. Esterowitz, R. Allen, and L. Aggarwal, *Electron. Lett.* **24**, 1104 (1988).
42. J.Y. Allain, M. Monerie, and H. Poignant, *Electron. Lett.* **25**, 1660 (1989).
43. J.N. Carter, R.G. Smart, D.C. Hanna, and A.C. Tropper, *Electron. Lett.* **26**, 1759 (1990).

44. R.M. Percival, S.F. Carter, D. Szebesta, S.T. Davey, and W.A. Stallard, *Electron. Lett.* **27**, 1912 (1991).
45. R.G. Smart, A.C. Tropper, D.C. Hanna, J.N. Carter, S.T. Davey, S.F. Carter, and D. Szebesta, *Electron. Lett.* **28**, 58 (1992).
46. J.N. Carter, R.G., Smart, A.C. Tropper, and D.C. Hanna, *J. Non-Cryst. Solids* **140**, 10 (1992).
47. J.Y. Allain, M. Monerie, and H. Poignant, *Electron. Lett.* **27**, 189 (1991).
48. Y. Ohishi, T. Terutoshi, and S. Takahasi, *IEEE Photo. Techn. Lett.* **3**, 688 (1991).
49. Y. Ohishi and T. Kanamori, *Electron. Lett.* **28**, 162 (1992).
50. M.C. Brieley, P.W. France, and C.A. Millar, *Electron. Lett.* **24**, 539 (1988).
51. L. Wetenkamp, *Electron. Lett.* **26**, 883 (1990).
52. J. Allain, M. Monerie, and H. Poignant, *Electron. Lett.* **27**, 1513 (1991).
53. R.G. Smart, J.N. Carter, A.C. Tropper, D.C. Hanna, S.F. Carter, and D. Szebesta, *J. Lightwave Techn.* **10**, 1702 (1991).
54. J.N. Carter, R.G. Smart, A.C. Tropper, D.C. Hanna, S.F. Carter, and D. Szebesta, *J. Lightwave Techn.* **9**, 1548 (1991).
55. Y. Ohoshi, K. Kanamori, T. Kitagawa, S. Takahashi, and E. Snitzer, *Opt. Lett.* **16**, 1747 (1991.)
56. Y. Durteste, M. Monerie, J.Y. Allain, and H. Poignant, *Electron. Lett.* **27**, 626 (1991).
57. S.F. Carter, D. Szebesta, S.T. Davey, R. Wyatt, M.C. Brierly, and P.W. France, *Electron. Lett.* **27**, 628 (1991).
58. J.Y. Allain, M. Monerie, and H. Poignat, *Electron. Lett.* **27**, 1012 (1991).
59. Y. Ohishi, T. Kanamori, and S. Takahashi, *IEEE Photo. Techn. Lett.* **3**, 715 (1991).
60. R. Lobbet, R. Wyatt, P. Eardley, P. Smyth, D. Szebasta, S.F. Carter, S.T. Davey, C.A. Davey, and M.C. Brieley, *Electron. Lett.* **27**, 1472 (1991.)
61. Y. Ohishi, T. Kanamori, J. Temmyo, M. Wada, M. Yamada, M. Shimizu, K. Yoshino, H. Hanafusa, M. Horiguchi, and S. Takahashi, *Electron. Lett.* **27**, 1995 (1991).
62. Y. Ohishi, T. Kanamori, T. Nishi, S. Takahashi, and E. Snitzer, *IEEE Trans. Photon. Techn. Lett.* **3**, 990 (1991).
63. Y. Miajima, T. Sugawa, and Y. Fukasaku, *Electron. Lett.* **27**, 1706 (1991).
64. M. Obro, J.E. Pedersen, and M.C. Brieley, *Electron. Lett.* **28**, 99 (1992).
65. D. Ronarc'h, M. Guibert, H. Ibrahim, M. Monerie, H. Poignant, and A. Tromeur, *Electron. Lett.* **27**, 908 (1991).
66. T.J. Witley, C.A. Millar, M.C. Brierly, and S.F. Carter, *Electron. Lett.* **27**, 184 (1991).
67. M. Zirngibl, *Electron. Lett.* **27**, 560 (1991).
68. M. Nakazawa, and Y. Kimura, *Electron. Lett.* **27**, 1065 (1991).
69. R.M. Percival, S. Cole, D.M. Cooper, S.P. Craig–Rayn, A.D. Ellis, C.J. Rowe, and W.A. Stallard, *Electron. Lett.* **27**, 1266 (1991).
70. B. Pedersen, S. Zemon, and W.J. Miniscalo, *Electron. Lett.* **27**, 1295 (1991).
71. J.E. Townsend, W.L. Barnes, and K.P. Jędrzejewski, *Electron. Lett.* **27**, 1958 (1991).
72. M. Ohashi, and K. Shiraki, *Electron. Lett.* **27**, 2143 (1991).
73. M. Horiguchi, M. Shimizu, M. Yamada, K. Yoshino, and H. Hanafusa, *Electron. Lett.* **27**, 2319 (1991).
74. R.S. Quimby, M.G. Drexhage, and M.J. Suscavage, *Electron. Lett.* **23**, 32 (1987).
75. J.Y. Allain, M. Monerie, and H. Poignant, *Electron. Lett.* **26**, 166 (1990).
76. J.Y. Allain, M. Monerie, and H. Poignant, *Electron. Lett.* **27**, 1156 (1991).
77. R.G. Smart, D.C. Hanna, A.C. Tropper, S.T. Davey, S.F. Carter, and D. Szebesta, *Electron. Lett.* **27**, 1307 (1991).
78. T.J. Whitley, C.A. Millar, R. Wyatt, M.C. Brierly, and D. Szebesta, *Electron. Lett.* **27**, 1785 (1991).
79. K. Hirao, S. Tanabe, S. Kishimoto, K. Tamai, and N. Soga, *J. Non-Cryst. Solids* **135**, 90 (1991).
80. J.Y. Allain, M. Monerie, and H. Poignant, *Electron. Lett.* **28**, 111 (1992).
81. K. Hirao, S. Todoroki, and N. Soga, *J. Non-Cryst. Solids* **143**, 40 (1992).
82. K. Binnemans, R.Van Deun, C. Gorller–Walrand, and J.L. Adam, *J. Alloys and Comp.* **275–277**, 455 (1998).
83. M. Tsuda, K. Soga, H. Inoue, and A. Makishima, *J. Appl. Physics* **85**, 29 (1999).
84. K. Tanimura, M.D. Shinn, W.A. Si1bley, M.G. Drexhage, and R.N. Brown, *Phys. Rev. B.* **30**, 2429 (1984).
85. R. Reisfel, R. Greenberg, R.N. Brown, M.G. Drexhage, and C.K. Jorsen, *Chem. Phys. Lett.* **95**, 91 (1983).
86. R.G. Smart, J.N. Carter, A.C. Tropper, D.C. Hanna, S.F. Carter, and D. Szebesta, *Electron. Lett.* **27**, 1123 (1991).
87. D. Ronarc'h, M. Guibert, H. Ibrahim, M. Monerie, H. Poignant, and A. Tromeur, *Electron. Lett.* **27**, 908 (1991).
88. H.M. Percival, D. Szebesta, S.T. Davey, N.A. Swain, and T.A. King, *Electron. Lett.* **28**, 2231 (1992).
89. S. Mitachi, T. Miyashita, and T. Kanamori, *Electron. Lett.* **17**, 591 (1981).
90. D.C. Tran, C.F. Fisher, and G.H. Sigel, *Electron. Lett.* **18**, 657 (1982).

